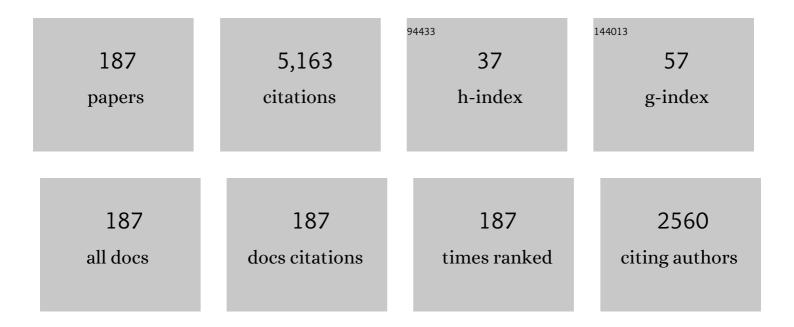
List of Publications by Year in descending order

Source: https://exaly.com/author-pdf/8872382/publications.pdf Version: 2024-02-01



ΜΑΡΟΊς ΔΙΟÃΩΝ

#	Article	IF	CITATIONS
1	Transition from saliva droplets to solid aerosols in the context of COVID-19 spreading. Environmental Research, 2022, 204, 112072.	7.5	27
2	Flame structure and burning velocity of ammonia/air turbulent premixed flames at high Karlovitz number conditions. Combustion and Flame, 2022, 238, 111943.	5.2	21
3	Structure and scalar correlation of ammonia/air turbulent premixed flames in the distributed reaction zone regime. Combustion and Flame, 2022, 241, 112090.	5.2	17
4	Ignition and combustion behavior of single micron-sized iron particle in hot gas flow. Combustion and Flame, 2022, 241, 112099.	5.2	22
5	Signal-enhanced Raman spectroscopy with a multi-pass cavity for quantitative measurements of formaldehyde, major species and temperature in a one-dimensional laminar DME-air flame. Combustion and Flame, 2022, 244, 112221.	5.2	7
6	Temporal temperature measurement on burning biomass pellets using phosphor thermometry and two-line atomic fluorescence. Proceedings of the Combustion Institute, 2021, 38, 3929-3938.	3.9	17
7	Optical characterization of methanol compression-ignition combustion in a heavy-duty engine. Proceedings of the Combustion Institute, 2021, 38, 5509-5517.	3.9	15
8	Numerical simulation of a mixed-mode reaction front in a PPC engine. Proceedings of the Combustion Institute, 2021, 38, 5703-5711.	3.9	5
9	Mid-infrared laser-induced thermal grating spectroscopy of hot water lines for flame thermometry. Proceedings of the Combustion Institute, 2021, 38, 1885-1893.	3.9	8
10	Suppression of unpolarized background interferences for Raman spectroscopy under continuous operation. Optics Express, 2021, 29, 1048.	3.4	10
11	Structure and Laminar Flame Speed of an Ammonia/Methane/Air Premixed Flame under Varying Pressure and Equivalence Ratio. Energy & Fuels, 2021, 35, 7179-7192.	5.1	60
12	Fiber-based stray light suppression in spectroscopy using periodic shadowing. Optics Express, 2021, 29, 7232.	3.4	7
13	Time-resolved polarization lock-in filtering for background suppression in Raman spectroscopy of biomass pyrolysis. Combustion and Flame, 2021, 224, 219-224.	5.2	5
14	Ultraviolet Absorption Cross-Sections of Ammonia at Elevated Temperatures for Nonintrusive Quantitative Detection in Combustion Environments. Applied Spectroscopy, 2021, 75, 1168-1177.	2.2	13
15	Investigation of laserâ€induced grating spectroscopy of O ₂ for accurate temperature measurements towards applications in harsh environments. Journal of Raman Spectroscopy, 2021, 52, 1569-1581.	2.5	2
16	Special Issue in Memory of Professor Mário Costa. Energy & Fuels, 2021, 35, 6935-6939.	5.1	0
17	Investigation of Fuel and Load Flexibility in a Siemens Gas Turbine-600/700/800 Burner Under Atmospheric Pressure Conditions Using High-Speed Hydroxyl-PLIF and Hydroxyl Radical Chemiluminescence Imaging. Journal of Engineering for Gas Turbines and Power, 2021, 143, .	1.1	2
18	Recent Development in Numerical Simulations and Experimental Studies of Biomass Thermochemical Conversion. Energy & Fuels, 2021, 35, 6940-6963.	5.1	45

#	Article	IF	CITATIONS
19	Clustering-based particle detection method for digital holography to detect the three-dimensional location and in-plane size of particles. Measurement Science and Technology, 2021, 32, 055205.	2.6	27
20	Investigation of turbulent premixed methane/air and hydrogen-enriched methane/air flames in a laboratory-scale gas turbine model combustor. International Journal of Hydrogen Energy, 2021, 46, 13377-13388.	7.1	32
21	Quantification of the size, 3D location and velocity of burning iron particles in premixed methane flames using high-speed digital in-line holography. Combustion and Flame, 2021, 230, 111430.	5.2	22
22	Stereoscopic high-speed imaging of iron microexplosions and nanoparticle-release. Optics Express, 2021, 29, 34465.	3.4	25
23	Airborne Gold Nanoparticle Detection Using Photoluminescence Excited with a Continuous Wave Laser. Applied Spectroscopy, 2021, 75, 1402-1409.	2.2	4
24	Simultaneous Quantitative Detection of HCN and C2H2 in Combustion Environment Using TDLAS. Processes, 2021, 9, 2033.	2.8	10
25	Investigating photomultiplier tube nonlinearities in high-speed phosphor thermometry using light emitting diode simulated decay curves. Review of Scientific Instruments, 2021, 92, 123102.	1.3	5
26	Structures of inverse jet flames stabilized on a coaxial burner. Energy, 2020, 193, 116757.	8.8	9
27	Flame investigations of a laboratory-scale CECOST swirl burner at atmospheric pressure conditions. Fuel, 2020, 279, 118421.	6.4	13
28	Dual-Laser-Induced Breakdown Thermometry via Sound Speed Measurement: A New Procedure for Improved Spatiotemporal Resolution. Sensors, 2020, 20, 2803.	3.8	4
29	A versatile, low-cost, snapshot multidimensional imaging approach based on structured light. Optics Express, 2020, 28, 9572.	3.4	18
30	Stabilization of a turbulent premixed flame by a plasma filament. Combustion and Flame, 2019, 208, 79-85.	5.2	25
31	Quantitative SO ₂ Detection in Combustion Environments Using Broad Band Ultraviolet Absorption and Laser-Induced Fluorescence. Analytical Chemistry, 2019, 91, 10849-10855.	6.5	24
32	Numerical simulation of ignition mode and ignition delay time of pulverized biomass particles. Combustion and Flame, 2019, 206, 400-410.	5.2	31
33	Layered structure around an extended gliding discharge column in a methane-nitrogen mixture at high pressure. Applied Physics Letters, 2019, 114, .	3.3	3
34	Ultraviolet Absorption Cross Sections of KOH and KCl for Nonintrusive Species-Specific Quantitative Detection in Hot Flue Gases. Analytical Chemistry, 2019, 91, 4719-4726.	6.5	25
35	Simultaneous 36†kHz PLIF/chemiluminescence imaging of fuel, CH2O and combustion in a PPC engine. Proceedings of the Combustion Institute, 2019, 37, 4751-4758.	3.9	27
36	Mid-Infrared Polarization Spectroscopy Measurements of Species Concentrations and Temperature in a Low-Pressure Flame. Applied Spectroscopy, 2019, 73, 653-664.	2.2	10

#	Article	IF	CITATIONS
37	Characteristics of a Gliding Arc Discharge Under the Influence of a Laminar Premixed Flame. IEEE Transactions on Plasma Science, 2019, 47, 403-409.	1.3	7
38	Two-photon-excited fluorescence of CO: experiments and modeling. Optics Express, 2019, 27, 25656.	3.4	8
39	Gain mechanism of femtosecond two-photon-excited lasing effect in atomic hydrogen. Optics Letters, 2019, 44, 2374.	3.3	8
40	Instantaneous imaging of ozone in a gliding arc discharge using photofragmentation laser-induced fluorescence. Journal Physics D: Applied Physics, 2018, 51, 135203.	2.8	10
41	Spatially Resolved Temperature Measurements Above a Burning Wood Pellet Using Diode Laser-Based Two-Line Atomic Fluorescence. Applied Spectroscopy, 2018, 72, 964-970.	2.2	12
42	Investigation of OH and CH2O distributions at ultra-high repetition rates by planar laser induced fluorescence imaging in highly turbulent jet flames. Fuel, 2018, 234, 1528-1540.	6.4	24
43	Formation of NO and NH in NH3-doped CH4 + N2 + O2 flame: Experiments and modelling. Combustion Flame, 2018, 194, 278-284.	and 5.2	16
44	Re-igniting the afterglow plasma column of an AC powered gliding arc discharge in atmospheric-pressure air. Applied Physics Letters, 2018, 112, .	3.3	11
45	Spectrally Resolved Ultraviolet (UV) Absorption Cross-Sections of Alkali Hydroxides and Chlorides Measured in Hot Flue Gases. Applied Spectroscopy, 2018, 72, 1388-1395.	2.2	18
46	Scheimpflug Lidar for combustion diagnostics. Optics Express, 2018, 26, 14842.	3.4	27
47	Femtosecond two-photon-excited backward lasing of atomic hydrogen in a flame. Optics Letters, 2018, 43, 1183.	3.3	18
48	Temporally and spectrally resolved images of single burning pulverized wheat straw particles. Fuel, 2018, 224, 434-441.	6.4	29
49	Gas Temperature Measurement Using Differential Optical Absorption Spectroscopy (DOAS). Applied Spectroscopy, 2018, 72, 1014-1020.	2.2	9
50	Simultaneous multispectral imaging of flame species using Frequency Recognition Algorithm for Multiple Exposures (FRAME). Combustion and Flame, 2018, 192, 160-169.	5.2	22
51	Effect of turbulent flow on an atmospheric-pressure AC powered gliding arc discharge. Journal of Applied Physics, 2018, 123, .	2.5	30
52	Spatiotemporally resolved characteristics of a gliding arc discharge in a turbulent air flow at atmospheric pressure. Physics of Plasmas, 2017, 24, .	1.9	50
53	In-Situ Non-intrusive Diagnostics of Toluene Removal by a Gliding Arc Discharge Using Planar Laser-Induced Fluorescence. Plasma Chemistry and Plasma Processing, 2017, 37, 433-450.	2.4	20
54	Direct numerical simulations of a high Karlovitz number laboratory premixed jet flame – an analysis of flame stretch and flame thickening. Journal of Fluid Mechanics, 2017, 815, 511-536.	3.4	114

#	Article	IF	CITATIONS
55	Quantitative Measurement of Atomic Potassium in Plumes over Burning Solid Fuels Using Infrared-Diode Laser Spectroscopy. Energy & Fuels, 2017, 31, 2831-2837.	5.1	34
56	Multi-species PLIF study of the structures of turbulent premixed methane/air jet flames in the flamelet and thin-reaction zones regimes. Combustion and Flame, 2017, 182, 324-338.	5.2	35
57	Simultaneous Visualization of Hydrogen Peroxide and Water Concentrations Using Photofragmentation Laser-Induced Fluorescence. Applied Spectroscopy, 2017, 71, 2118-2127.	2.2	3
58	Online Alkali Measurement during Oxy-fuel Combustion. Energy Procedia, 2017, 120, 365-372.	1.8	7
59	FRAME: femtosecond videography for atomic and molecular dynamics. Light: Science and Applications, 2017, 6, e17045-e17045.	16.6	103
60	Characterization of an AC glow-type gliding arc discharge in atmospheric air with a current-voltage lumped model. Physics of Plasmas, 2017, 24, .	1.9	30
61	A novel multi-jet burner for hot flue gases of wide range of temperatures and compositions for optical diagnostics of solid fuels gasification/combustion. Review of Scientific Instruments, 2017, 88, 045104.	1.3	34
62	Numerical and Experimental Study on Laminar Methane/Air Premixed Flames at Varying Pressure. Energy Procedia, 2017, 105, 4970-4975.	1.8	5
63	Experimental investigations of potassium chemistry in premixed flames. Fuel, 2017, 203, 802-810.	6.4	19
64	Strategy for improved NH 2 detection in combustion environments using an Alexandrite laser. Spectrochimica Acta - Part A: Molecular and Biomolecular Spectroscopy, 2017, 184, 235-242.	3.9	17
65	Quantitative Imaging of Ozone Vapor Using Photofragmentation Laser-Induced Fluorescence (LIF). Applied Spectroscopy, 2017, 71, 1578-1585.	2.2	6
66	Diode laser-based thermometry using two-line atomic fluorescence of indium and gallium. Applied Physics B: Lasers and Optics, 2017, 123, 278.	2.2	33
67	Laser-Induced Photofragmentation Fluorescence Imaging of Alkali Compounds in Flames. Applied Spectroscopy, 2017, 71, 1289-1299.	2.2	18
68	Thin reaction zone and distributed reaction zone regimes in turbulent premixed methane/air flames: Scalar distributions and correlations. Combustion and Flame, 2017, 175, 220-236.	5.2	72
69	Mid-infrared laser-induced thermal grating spectroscopy in flames. Proceedings of the Combustion Institute, 2017, 36, 4515-4523.	3.9	18
70	Instantaneous 3D imaging of flame species using coded laser illumination. Proceedings of the Combustion Institute, 2017, 36, 4585-4591.	3.9	35
71	Simultaneous Burst Imaging of Dual Species Using Planar Laser-Induced Fluorescence at 50 kHz in Turbulent Premixed Flames. Applied Spectroscopy, 2017, 71, 1363-1367.	2.2	13
72	Translational, rotational, vibrational and electron temperatures of a gliding arc discharge. Optics Express, 2017, 25, 20243.	3.4	77

#	Article	IF	CITATIONS
73	Ultra-high-speed PLIF imaging for simultaneous visualization of multiple species in turbulent flames. Optics Express, 2017, 25, 30214.	3.4	39
74	Setup for microwave stimulation of a turbulent low-swirl flame. Journal Physics D: Applied Physics, 2016, 49, 185601.	2.8	8
75	Misalignment Effects in Laser-Induced Grating Experiments. Applied Spectroscopy, 2016, 70, 2025-2028.	2.2	3
76	Two-dimensional OH-thermometry in reacting flows using photofragmentation laser-induced florescence. Combustion and Flame, 2016, 169, 297-306.	5.2	13
77	Investigation of photochemical effects in flame diagnostics with picosecond photofragmentation laser-induced fluorescence. Combustion and Flame, 2016, 171, 59-68.	5.2	2
78	Investigation of the effect of engine lubricant oil on remote temperature sensing using thermographic phosphors. Journal of Luminescence, 2016, 179, 568-573.	3.1	5
79	Mid-Infrared Pumped Laser-Induced Thermal Grating Spectroscopy for Detection of Acetylene in the Visible Spectral Range. Applied Spectroscopy, 2016, 70, 1034-1043.	2.2	15
80	Remote temperature sensing on and beneath atmospheric plasma sprayed thermal barrier coatings using thermographic phosphors. Surface and Coatings Technology, 2016, 302, 359-367.	4.8	14
81	Temperature imaging in low-pressure flames using diode laser two-line atomic fluorescence employing a novel indium seeding technique. Applied Physics B: Lasers and Optics, 2016, 122, 1.	2.2	17
82	Investigation of roâ€vibrational spectra of small hydrocarbons at elevated temperatures using infrared degenerate fourâ€wave mixing. Journal of Raman Spectroscopy, 2016, 47, 1130-1139.	2.5	8
83	Structure of premixed ammoniaÂ+Âair flames at atmospheric pressure: Laser diagnostics and kinetic modeling. Combustion and Flame, 2016, 163, 370-381.	5.2	83
84	Single-shot, planar infrared imaging in flames using polarization spectroscopy. Optics Express, 2015, 23, 30414.	3.4	4
85	Single-shot photofragment imaging by structured illumination. Optics Letters, 2015, 40, 5019.	3.3	9
86	Advancements in Rayleigh scattering thermometry by means of structured illumination. Proceedings of the Combustion Institute, 2015, 35, 3689-3696.	3.9	49
87	Development and application of CN PLIF for single-shot imaging in turbulent flames. Combustion and Flame, 2015, 162, 368-374.	5.2	11
88	Real-Time Gas-Phase Imaging over a Pd(110) Catalyst during CO Oxidation by Means of Planar Laser-Induced Fluorescence. ACS Catalysis, 2015, 5, 2028-2034.	11.2	26
89	Investigation of formaldehyde enhancement by ozone addition in CH4/air premixed flames. Combustion and Flame, 2015, 162, 1284-1293.	5.2	22
90	Analysis of in-cylinder H2O2 and HO2 distributions in an HCCI engine – Comparison of laser-diagnostic results with CFD and SRM simulations. Combustion and Flame, 2015, 162, 3131-3139.	5.2	25

#	Article	IF	CITATIONS
91	Experimental apparatus with full optical access for combustion experiments with laminar flames from a single circular nozzle at elevated pressures. Review of Scientific Instruments, 2015, 86, 035115.	1.3	12
92	Investigation of Hydrogen Enriched Natural Gas Flames in a SGT-700/800 Burner Using OH PLIF and Chemiluminescence Imaging. Journal of Engineering for Gas Turbines and Power, 2015, 137, .	1.1	21
93	Time-resolved spectroscopic study of photofragment fluorescence in methane/air mixtures and its diagnostic implications. Applied Physics B: Lasers and Optics, 2015, 120, 587-599.	2.2	6
94	Visualization of multi-regime turbulent combustion in swirl-stabilized lean premixed flames. Combustion and Flame, 2015, 162, 2954-2958.	5.2	31
95	Numerical and experimental study of flame propagation and quenching of lean premixed turbulent low swirl flames at different Reynolds numbers. Combustion and Flame, 2015, 162, 2582-2591.	5.2	13
96	Distributed reactions in highly turbulent premixed methane/air flames. Combustion and Flame, 2015, 162, 2937-2953.	5.2	117
97	Spatially and temporally resolved gas distributions around heterogeneous catalysts using infrared planar laser-induced fluorescence. Nature Communications, 2015, 6, 7076.	12.8	41
98	Sustained diffusive alternating current gliding arc discharge in atmospheric pressure air. Applied Physics Letters, 2014, 105, .	3.3	58
99	Stray light suppression in spectroscopy using periodic shadowing. Optics Express, 2014, 22, 7711.	3.4	43
100	Low-noise mid-IR upconversion detector for improved IR-degenerate four-wave mixing gas sensing. Optics Letters, 2014, 39, 5321.	3.3	47
101	Simultaneous one-dimensional fluorescence lifetime measurements of OH and CO in premixed flames. Applied Physics B: Lasers and Optics, 2014, 115, 35-43.	2.2	13
102	Lll–lidar: range-resolved backward picosecond laser-induced incandescence. Applied Physics B: Lasers and Optics, 2014, 115, 111-121.	2.2	12
103	Characterization of ammonia two-photon laser-induced fluorescence for gas-phase diagnostics. Applied Physics B: Lasers and Optics, 2014, 115, 25-33.	2.2	20
104	A library-based algorithm for evaluation of luminescent decay curves by shape recognition in time domain phosphor thermometry. Journal of Thermal Analysis and Calorimetry, 2014, 115, 545-554.	3.6	7
105	Stability of alternating current gliding arcs. European Physical Journal D, 2014, 68, 1.	1.3	16
106	Dynamics, OH distributions and UV emission of a gliding arc at various flow-rates investigated by optical measurements. Journal Physics D: Applied Physics, 2014, 47, 295203.	2.8	72
107	Time-resolved (kHz) 3D imaging of OH PLIF in a flame. Experiments in Fluids, 2014, 55, 1.	2.4	48
108	Large eddy simulations and rotational CARS/PIV/PLIF measurements of a lean premixed low swirl stabilized flame. Combustion and Flame, 2014, 161, 2539-2551.	5.2	15

#	Article	IF	CITATIONS
109	Strategy for PLIF single-shot HCO imaging in turbulent methane/air flames. Combustion and Flame, 2014, 161, 1566-1574.	5.2	37
110	Two-pulse structured illumination imaging. Optics Letters, 2014, 39, 2584.	3.3	35
111	Laser-Induced Fluorescence Detection of Hot Molecular Oxygen in Flames Using an Alexandrite Laser. Applied Spectroscopy, 2014, 68, 1266-1273.	2.2	2
112	Simultaneous Visualization of Water and Hydrogen Peroxide Vapor Using Two-Photon Laser-Induced Fluorescence and Photofragmentation Laser-Induced Fluorescence. Applied Spectroscopy, 2014, 68, 1333-1341.	2.2	7
113	Quantitative oxygen concentration imaging in toluene atmospheres using Dual Imaging with Modeling Evaluation. Experiments in Fluids, 2013, 54, 1.	2.4	5
114	Room-Fire Characterization Using Highly Range-Resolved Picosecond Lidar Diagnostics and CFD Simulations. Combustion Science and Technology, 2013, 185, 749-765.	2.3	9
115	Thickness dependent variations in surface phosphor thermometry during transient combustion in an HCCI engine. Combustion and Flame, 2013, 160, 1466-1475.	5.2	40
116	Water-cooled non-thermal gliding arc for adhesion improvement of glass-fibre-reinforced polyester. Journal Physics D: Applied Physics, 2013, 46, 135203.	2.8	38
117	Post-flame gas-phase sulfation of potassium chloride. Combustion and Flame, 2013, 160, 959-969.	5.2	72
118	Picosecond excitation for reduction of photolytic effects in two-photon laser-induced fluorescence of CO. Proceedings of the Combustion Institute, 2013, 34, 3541-3548.	3.9	22
119	In-situ Measurement of Sodium and Potassium Release during Oxy-Fuel Combustion of Lignite using Laser-Induced Breakdown Spectroscopy: Effects of O ₂ and CO ₂ Concentration. Energy & Fuels, 2013, 27, 1123-1130.	5.1	97
120	Atmospheric Pressure Acetylene Detection by UV Photo-Fragmentation and Induced C ₂ Emission. Applied Spectroscopy, 2013, 67, 66-72.	2.2	4
121	Comparison of Three Schemes of Two-Photon Laser-Induced Fluorescence for CO Detection in Flames. Applied Spectroscopy, 2013, 67, 314-320.	2.2	21
122	Highly range-resolved ammonia detection using near-field picosecond differential absorption lidar. Optics Express, 2012, 20, 20688.	3.4	15
123	Single-laser shot fluorescence lifetime imaging on the nanosecond timescale using a Dual Image and Modeling Evaluation algorithm. Optics Express, 2012, 20, 3043.	3.4	20
124	Laser-induced breakdown flame thermometry. Combustion and Flame, 2012, 159, 3576-3582.	5.2	63
125	PLIF diagnostics of NO oxidization and OH consumption in pulsed corona discharge. Fuel, 2012, 102, 729-736.	6.4	10
126	MD2-3 Quantitative in-cylinder fuel measurements in a heavy duty diesel engine using Structured Laser Illumination Planar Imaging (SLIPI)(MD: Measurement and Diagnostics,General Session Papers). The Proceedings of the International Symposium on Diagnostics and Modeling of Combustion in Internal Combustion Engines, 2012, 2012.8, 500-505.	0.1	6

#	Article	IF	CITATIONS
127	Cl2-2 Liquid Spray Penetration Length during Late Post Injection in an Optical Light-Duty Diesel Engine(Cl: Compression Ignition Engine Combustion,General Session Papers). The Proceedings of the International Symposium on Diagnostics and Modeling of Combustion in Internal Combustion Engines, 2012, 2012.8, 206-211.	0.1	1
128	Sodium and Potassium Released from Burning Particles of Brown Coal and Pine Wood in a Laminar Premixed Methane Flame Using Quantitative Laser-Induced Breakdown Spectroscopy. Applied Spectroscopy, 2011, 65, 684-691.	2.2	68
129	Time resolved, 3D imaging (4D) of two phase flow at a repetition rate of 1 kHz. Optics Express, 2011, 19, 21508.	3.4	34
130	Extinction coefficient imaging of turbid media using dual structured laser illumination planar imaging. Optics Letters, 2011, 36, 1656.	3.3	28
131	Thermographic phosphors for thermometry: A survey of combustion applications. Progress in Energy and Combustion Science, 2011, 37, 422-461.	31.2	245
132	Three-dimensional measurement of the local extinction coefficient in a dense spray. Measurement Science and Technology, 2011, 22, 125303.	2.6	27
133	Picosecond-lidar thermometry in a measurement volume surrounded by highly scattering media. Measurement Science and Technology, 2011, 22, 125302.	2.6	17
134	Detection of Flame Radicals Using Light-Emitting Diodes. Applied Spectroscopy, 2010, 64, 1330-1334.	2.2	11
135	Two-dimensional thermometry using temperature-induced line shifts of ZnO:Zn and ZnO:Ga fluorescence. Optics Letters, 2008, 33, 1327.	3.3	46
136	Application of structured illumination for multiple scattering suppression in planar laser imaging of dense sprays. Optics Express, 2008, 16, 17870.	3.4	148
137	Investigations of blue emitting phosphors for thermometry. Measurement Science and Technology, 2008, 19, 125304.	2.6	51
138	Simultaneous laser-induced fluorescence and sub-Doppler polarization spectroscopy of the CH radical. Optics Communications, 2007, 270, 347-352.	2.1	28
139	QUANTITATIVE MEASUREMENTS OF SPECIES AND TEMPERATURE IN A DME-AIR COUNTERFLOW DIFFUSION FLAME USING LASER DIAGNOSTIC METHODS. Combustion Science and Technology, 2006, 178, 1165-1184.	2.3	22
140	Studies of the Combustion Process with Simultaneous Formaldehyde and OH PLIF in a Direct-Injected HCCI Engine. JSME International Journal Series B, 2005, 48, 701-707.	0.3	22
141	Strategies for Formaldehyde Detection in Flames and Engines Using a Single-Mode Nd:YAG/OPO Laser System. Applied Spectroscopy, 2005, 59, 763-768.	2.2	17
142	Temperature measurements of combustible and non-combustible surfaces using laser induced phosphorescence. Experimental Thermal and Fluid Science, 2004, 28, 669-676.	2.7	51
143	Chemiluminescence sensor for local equivalence ratio of reacting mixtures of fuel and air (FLAMESEEK). Applied Thermal Engineering, 2004, 24, 1619-1632.	6.0	69
144	Laser techniques in acoustically levitated micro droplets. Lab on A Chip, 2004, 4, 287-291.	6.0	62

#	Article	IF	CITATIONS
145	Optical and Mass Spectrometric Study of the Pyrolysis Gas of Wood Particles. Applied Spectroscopy, 2003, 57, 216-222.	2.2	24
146	Spark ignition of turbulent methane/air mixtures revealed by time-resolved planar laser-induced fluorescence and direct numerical simulations. Proceedings of the Combustion Institute, 2000, 28, 399-405.	3.9	73
147	Multipoint temperature and oxygen-concentration measurements using rotational coherent anti-Stokes Raman spectroscopy. Optics Letters, 2000, 25, 1535.	3.3	14
148	Laser spectroscopic techniques for combustion diagnostics. Combustion Science and Technology, 1999, 149, 1-18.	2.3	8
149	Stray light rejection in rotational coherent anti-Stokes Raman spectroscopy by use of a sodium-seeded flame. Applied Optics, 1998, 37, 8392.	2.1	15
150	Two-Dimensional Two-Phase Water Detection Using a Tunable Excimer Laser. Applied Spectroscopy, 1998, 52, 343-347.	2.2	4
151	Two-Dimensional Imaging of Flame Species Using Two-Photon Laser-Induced Fluorescence. Applied Spectroscopy, 1997, 51, 1229-1237.	2.2	31
152	Developments of laser-induced fluorescence for two-dimensional multi-species imaging in flames. Spectrochimica Acta, Part B: Atomic Spectroscopy, 1997, 52, 1105-1112.	2.9	9
153	Simultaneous detection of OH and NO in a flame using polarization spectroscopy. Optics Communications, 1996, 124, 251-257.	2.1	11
154	Two-photon induced polarization spectroscopy applied to the detection of NH3 and CO molecules in cold flows and flames. Optics Communications, 1995, 114, 76-82.	2.1	29
155	Combined Vibrational and Rotational CARS for Simultaneous Measurements of Temperature and Concentrations of Fuel, Oxygen, and Nitrogen. Applied Spectroscopy, 1995, 49, 188-192.	2.2	39
156	Development and demonstration of 2D-LIF for studies of mixture preparation in SI engines. Combustion and Flame, 1994, 99, 449-457.	5.2	88
157	Developments of the amplified stimulated emission technique for spatially resolved species detection in flames. Optics Communications, 1994, 108, 71-76.	2.1	19
158	Two-photon laser-induced fluorescence and stimulated emission measurements from oxygen atoms in a hydrogen/oxygen flame with picosecond resolution. Optics Communications, 1994, 113, 315-323.	2.1	17
159	Measurements of the Collisionally Quenched Lifetime of CO in Hydrocarbon Flames. Applied Spectroscopy, 1994, 48, 1118-1124.	2.2	19
160	Application of a Prism Dye Laser for Enhanced Single-Shot CARS Intensities. Applied Spectroscopy, 1993, 47, 857-859.	2.2	0
161	A test of different rotational Raman linewidth models: Accuracy of rotational coherent anti‣tokes Raman scattering thermometry in nitrogen from 295 to 1850 K. Journal of Chemical Physics, 1993, 99, 2466-2477.	3.0	103
162	Rotational CARS Thermometry in Sooting Flames. Combustion Science and Technology, 1992, 81, 129-140.	2.3	47

#	Article	IF	CITATIONS
163	Detection of CO molecules using two-photon degenerate four-wave mixing (DFWM). Optics Communications, 1992, 94, 99-102.	2.1	22
164	Measurement of the collision-quenched lifetime of CO molecules in a flame at atmospheric pressure. Chemical Physics Letters, 1992, 189, 211-216.	2.6	26
165	Detection of nitrogen atoms in flames using two-photon laser-induced fluorescence and investigations of photochemical effects. Applied Optics, 1991, 30, 2990.	2.1	19
166	C2Production and Excitation in Sooting Flames using Visible Laser Radiation: Implications for Diagnostics in Sooting Flames. Combustion Science and Technology, 1991, 77, 307-318.	2.3	29
167	Vibrational CARS thermometry in sooty flames: Quantitative evaluation of C2 absorption interference. Combustion and Flame, 1990, 82, 199-210.	5.2	53
168	Optical investigation of laser-produced C2 in premixed sooty ethylene flames. Combustion and Flame, 1990, 80, 322-328.	5.2	46
169	Detection of atomic nitrogen using two-photon laser-induced stimulated emission: Application to flames. Chemical Physics Letters, 1990, 170, 406-410.	2.6	35
170	Laser-Induced Fluorescence Detection of NH3 in Flames with the Use of Two-Photon Excitation. Applied Spectroscopy, 1990, 44, 881-886.	2.2	30
171	Detection of carbon atoms in flames using stimulated emission induced by two-photon laser excitation. Optics Communications, 1989, 71, 263-268.	2.1	41
172	Spatially resolved flow velocity measurements using laser-induced fluorescence from a pulsed laser. Optics Letters, 1989, 14, 9.	3.3	15
173	Two-photon-excited stimulated emission from atomic oxygen in flames and cold gases. Optics Letters, 1989, 14, 305.	3.3	93
174	Detection of nitrogen molecules through multi-photon laser excitation and N+2 fluorescence. Optics Communications, 1988, 69, 31-36.	2.1	24
175	Application of Emission and Absorption Spectroscopy for Characterization of a Copper Converting Process. Applied Spectroscopy, 1988, 42, 128-133.	2.2	4
176	Application of CARS Spectroscopy to the Detection of SO2. Applied Spectroscopy, 1988, 42, 1421-1427.	2.2	3
177	Soot particle measurements in premixed ethylene flames using a pulsed laser method. Journal of Aerosol Science, 1988, 19, 959-962.	3.8	7
178	Spatially resolved flow velocity measurements using laser-induced fluorescence from a pulsed laser. Journal of Aerosol Science, 1988, 19, 963-965.	3.8	0
179	Simultaneous spatially resolved NO and NO_2 measurements using one- and two-photon laser-induced fluorescence. Optics Letters, 1985, 10, 529.	3.3	28
180	Analysis of the Correlation Between Engine-Out Particulates and Local Φ in the Lift-Off Region of a Heavy Duty Diesel Engine Using Raman Spectroscopy. SAE International Journal of Fuels and Lubricants, 0, 2, 645-660.	0.2	37

#	Article	IF	CITATIONS
181	Analysis of EGR Effects on the Soot Distribution in a Heavy Duty Diesel Engine using Time-Resolved Laser Induced Incandescence. SAE International Journal of Engines, 0, 3, 137-155.	0.4	21
182	Challenges for In-Cylinder High-Speed Two-Dimensional Laser-Induced Incandescence Measurements of Soot. SAE International Journal of Engines, 0, 4, 1607-1622.	0.4	18
183	Laser-Induced Phosphorescence and the Impact of Phosphor Coating Thickness on Crank-Angle Resolved Cylinder Wall Temperatures. SAE International Journal of Engines, 0, 4, 1689-1698.	0.4	35
184	Air-Entrainment in Wall-Jets Using SLIPI in a Heavy-Duty Diesel Engine. SAE International Journal of Engines, 0, 5, 1684-1692.	0.4	11
185	Study of the Early Flame Development in a Spark-Ignited Lean Burn Four-Stroke Large Bore Gas Engine by Fuel Tracer PLIF. SAE International Journal of Engines, 0, 7, 928-936.	0.4	13
186	Transition from HCCI to PPC: Investigation of Fuel Distribution by Planar Laser Induced Fluorescence (PLIF). SAE International Journal of Engines, 0, 10, 1465-1481.	0.4	18
187	Non-thermal gliding arc discharge assisted turbulent combustion (up to 80 kW) at extended conditions: phenomenological analysis. Combustion Science and Technology, 0, , 1-16.	2.3	1